CONF-8506152--2

DE85 014963

JUL 25 1985

CONF-8506152--2

DEEP INELASTIC MUON SCATTERING WITH HADRON DETECTION

D. F. Geesaman and M. C. Green
Argonne National Laboratory, Argonne, Illinois 60439

ABSTRACT

The physics motivation and experimental apparatus of FNAL E665 are described. E665 is a new experiment to study the hadrons in coincidence with muons deep inelastically scattered from nuclei. One of the goals of the experiment is to examine nuclear medium effects not only on the baryon quark distributions (the EMC effect) but also on the process of hadronization in high energy collisions.

Nuclear Physics has always been concerned with many-body effects in strongly interacting systems. Yet only in recent experiments[1,2,3] on deep inelastic scattering of leptons from nuclei has conclusive evidence been obtained that the nuclear medium has a significant effect on the quark structure of nuclei. The understanding of these phenomena should provide crucial insight in understanding the role of quark structure and quantumchromodynamics (QCD) in nuclei and the nonperturbative mechanism of confinement in QCD.

While confinement may arise naturally in QCD, the consequences of confinement for the structure of hadrons are not well understood at either low or high momentum transfer. An essential link has yet to be provided between the well understood electroweak interactions with the quarks and the physical hadrons that are detected in detectors and serve as the targets. Experiment 665 at Fermilab is designed[4] to address many of these issues from the static effects of the nuclear medium on quark distribution functions to the dynamic properties of hadron formation in high energy reactions. It can do this by combining the world's highest energy muon beam with a detector that is designed to provide efficient hadron detection and perhaps most important, excellent particle identification.

There is little question that electromagnetic (as well as weak) probes interact only with the quarks in nuclear matter. At sufficiently high momentum transfer, the successful parton model, justified by the asymtopic freedom of QCD, describes all observables in terms of the quark distribution functions. The cross section for inclusive muon or electron scattering is:

$$\frac{d\sigma}{dQ^2dx} = \frac{4\pi\alpha^2}{Q^4}\left[(1-y-\frac{M_p xy}{2E})\frac{F_2(x,Q^2)}{x} + y^2F_1(x,Q^2)\right] \qquad (1)$$

$$= \frac{4\pi\alpha^2}{Q^4} F_2(x,Q^2)\left[1-y-\frac{M_p xy}{4E(1+R(x,Q^2))}y^2(1+4\frac{M_p^2x^2}{Q^2})\right]$$

$$R = \frac{\sigma_L}{\sigma_T} = \left[(1+\frac{4M_p x^2}{Q^2})F_2-2xF_1\right]/2xF_1$$

$$x = \frac{Q^2}{2M_p(E-E')}$$

$$y = \frac{E-E'}{E}$$

x, as usual, represents the fraction of the hadron's momentum carried by each quark, E(E') is the initial (final) laboratory energy of the outgoing muon, and R is the ratio of longitudinal to transverse structure functions. The Q^2 dependence of F_1 and F_2 arises due to scale violations and is well described by QCD. This Q^2 dependence will not be explicitly indicated in the following expressions. The structure function F_2 is given in terms of the quark distribution functions by:

$$F_2(x) = \sum_i x\, e_i^2 f_i(x) \qquad (2)$$

where e_i is the charge for each flavor of quark, $f_i(x)$ is the x distribution of each flavor and the sum is over all quark flavors.

Figure 1 shows a summary of the comparison of muon and electron scattering on iron and deuterium. The EMC effect, the fact that the ratio of iron to deuterium is not one, immediately requires that (as long as the data are at sufficient momentum transfer that the parton

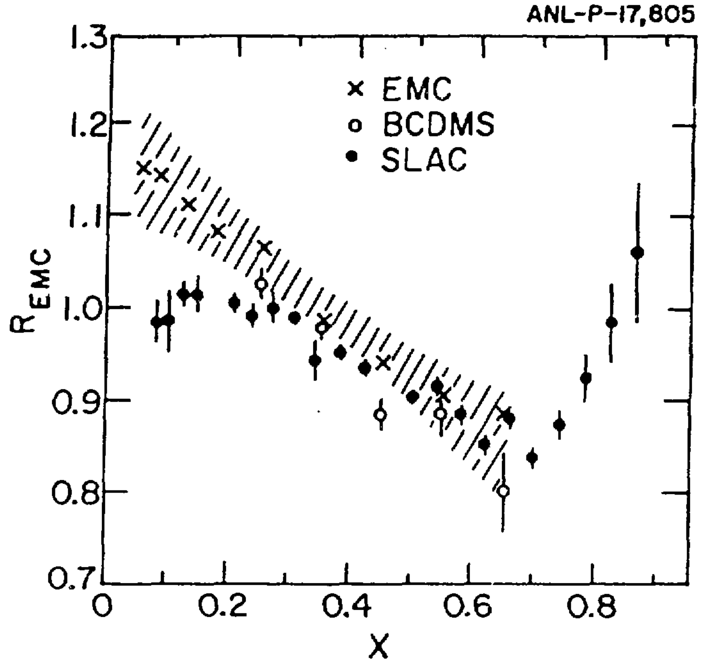

Figure 1 Compilation of the data on the ratio of structure functions F_2^{Fe}/F_2^D for deep inelastic muon and electron scattering. Results are shown from EMC (Ref. 1), BCDMS (Ref. 5) and SLAC (Ref. 3). For the SLAC data, the ratio σ^{Fe}/σ^D is shown. This is equivalent to F_2^{Fe}/F_2^D if R is not a function of A.

model applies) the distributions of quarks are different in iron and deuterium. Given these data, no one questions that the quark distributions are different; what is uncertain is which of the dozens of models active physicists have proposed to reproduce this data is indeed the correct one.

The differences between the data sets in Figure 1 draw a great deal of attention. The original EMC data have an additional uncertainty in the overall relative normalization of the iron and deuterium data of 7%. The agreement is certainly better if the EMC data are reduced by roughly 5%. There is an additional theoretical argument that the EMC data should be reduced by this amount based on the belief that the approach to asymtopia must be monotonic.[6] On the other hand, the SLAC data are taken at sufficiently low momentum transfer (particularly for small x) that the importance of effects of higher order in $1/Q^2$ and the contribution of the longitudinal structure function[7] are not well established. At this time, the structure functions at small x, < .2, must still be regarded as uncertain.

The explanations of the EMC effect have littered the journals much like fans litter the field at a White Sox game. They fall into there general classes. The first class attributes the EMC effect to a modification of the structure of the nucleon in the nucleus, a size change for example. The second class includes other hadronic objects in addition to nucleons in the nucleus. These other objects may be as conventional as pions or far more exotic. In the third class, the quarks are not confined to a single baryon, but may be shared between baryons (percolation). A conservative example from each of the first two classes is shown in Fig. 2. The solid curve represents the rescaling argument of Close et al.[8] that the structure functions of iron look like the structure functions of deuterium at a larger momentum transfer. The dashed curve is the calculation[9] of Berger and Coester[9] for a nucleus made up of nucleons and pions with the pion distribution determined from a two-body nucleon-nucleon interaction. (They only calculate the excess pions in the nucleus, not the usual pion cloud of the nucleon which is included in the empirical nucleon structure function.) One remarkable observation is that these two rather different physical processes give rather similar x dependences for the ratio of the iron and deuterium structure functions. Unless a significant A dependence is observed in R, the ratio of σ_L/σ_T, singles measurements of deep inelastic lepton scattering are not likely to provide substantial additional information on the underlying mechanism of the EMC effect.[10]

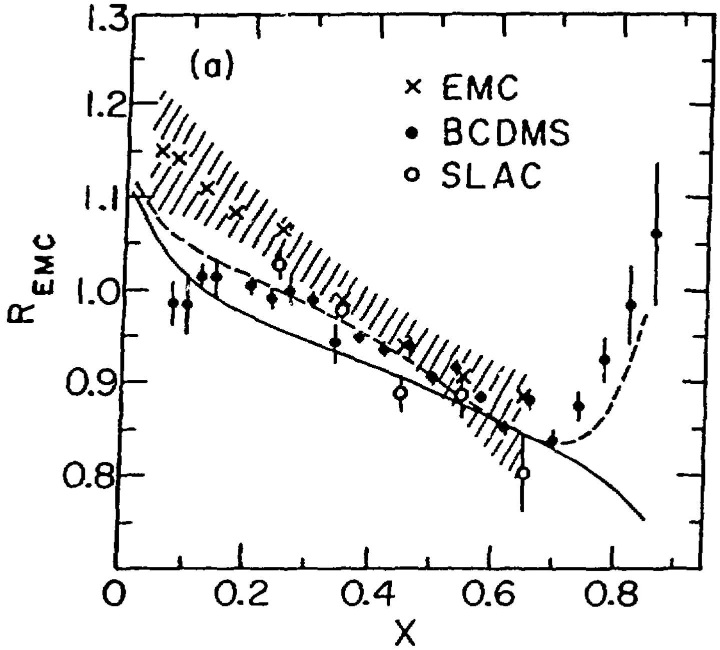

Figure 2 The data for F_2^{Fe}/F_2^{D} are compared to the rescaling prescription (solid curve, Ref. 8 evaluated for Q^2 appropriate to the muon data) and the inclusion of the excess pion distribution in nuclei (dashed curve, Ref. 9). This figure is taken from Ref. 9.

The CEBAF C.W. electron accelerator is dedicated to the concept that combining the clean electromagnetic probe with the power of coincidence experiments provides an extremely powerful tool in understanding nuclear dynamics. In the exact same spirit, E665 at FNAL extends the lepton deep inelastic scattering experiments by emphasizing the detection of the coincident hadrons. The configuration of the experimental equipment is illustrated in Fig. 3. The experiment conceptually divides into two correlated systems. The vertex detector consists of a streamer chamber and a superconducting vertex magnet, two threshold Cerenkov counters, wire chambers for track detection, and a time-of-flight system to measure wide angle particles. This system is designed to provide virtually 4π hadron detection for low energy hadrons. The second system, the forward spectrometer consists of the 8 Tesla-meter superconducting Chicago Cyclotron Magnet, an electromagnetic calorimeter to detect neutral particles, a ring imaging Cerenkov counter (RICH), drift and proportional wire chambers for track detection, and, following 6 m of steel absorber, a muon trigger. The RICH counter is a particularly significant part of the apparatus. By measuring the radius of the rings of Cerenkov light and accurately determining the trajectory of the track in upstream and downstream drift chambers, pions, kaons and protons can be separated up to momenta of 150 GeV/c.

FERMILAB E665 MUON SPECTROMETER

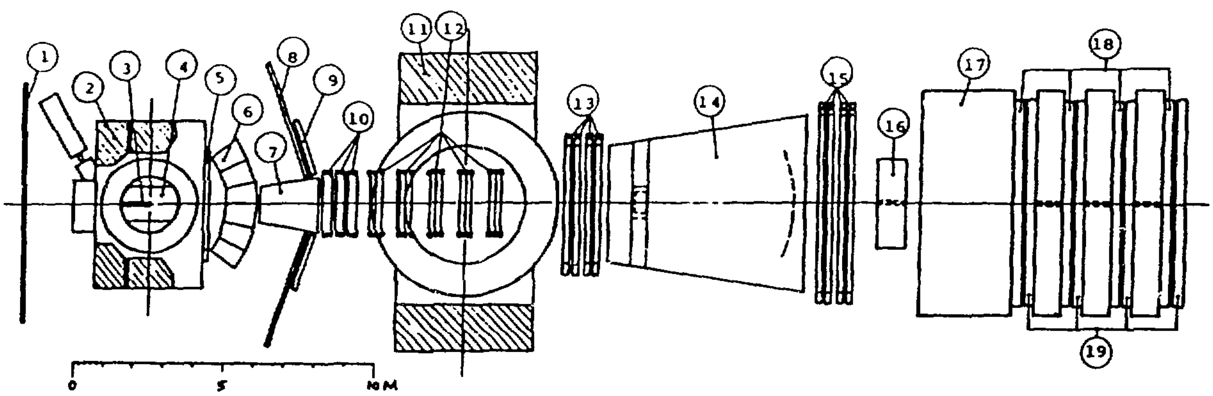

1. 7Mx3M Veto Counter Wall
2. CERN Vertex Magnet
3. 1M LH_2/LD_2 Target
4. 1Mx2Mx0.7M Streamer Chamber
5. 3Mx1M MWPC, 6 Planes
6. 144Cell Threshold Cerenkov Cntr
7. 58 Cell Threshold Cerenkov Cntr
8. 4Mx1.6M Scintillation TOF Arrays
9. 2Mx2M Prop. Drift Tube Arrays 4 Planes
10. 2Mx2M MWPC, 12 Planes
11. Chicago Cyclotron Magnet
12. 2Mx1M MWPC, 15 Planes
13. 4Mx2M Drift Chambers, 8 Planes
14. Ring Imaging Cerenkov Counter
15. 6Mx2M Drift Chambers, 8 Planes
16. 3Mx3M EM Shower Calorimeter
17. 7Mx3Mx3M Iron Absorber
18. 7Mx3M Prop. Tube Arrays, 8 Planes
19. 7Mx3M Scintillation Trigger Arrays

Figure 3 The experimental apparatus for FNAL E665.

An essential feature of the experiment is the new muon beam line which is being constructed at Fermilab. This beam line will provide a high quality muon beam at energies up to 800 GeV/c, more than 3 times the energy of the CERN muon experiments. Furthermore, since the muon channel can be configured to accept particular orientations of pion decay, a polarized muon beam can be provided at somewhat reduced intensity. This feature opens an exciting world of new "spin physics" to be exploited in future experiments.

There is the usual penalty to be paid in coincidence experiments. The target must be thin enough so that the emerging hadron momentum is not degraded either in magnitude or in direction. The streamer chamber provides the additional constraint that the targets should be dielectrics. Measurements are planned on 1m long liquid Hydrogen, Deuterium, Nitrogen and Xenon targets with typically 10^{12} muons incident for each target. With this luminosity the number of coincident hadron events will be roughly 30 times that seen in EMC coincidence measurements[11] which did not have the excellent particle identification.

There are many physics issues which E665 will address. These include new measurments of structure functions at small x, gluon jet phenomena, and the development of jets in nuclei. The high beam energy of the Tevatron muon beam translates into the ability to study phenomena at factors of 3 lower values of x than previous experiments while retaining sufficient momentum transfer for the parton model to apply. The increase in energy also makes jet structure much more readily discernable. These data will provide an important body of information on perturbative QCD interations.

It is appropriate to concentrate on two complementary aspects of the experiment which are uniquely nuclear physics. The first is the A dependence of hadrons which carry off most of the energy and momentum of the virtual photon, the so-called leading hadrons. This directly addresses the subject which excited the interest in this field: what is the mechanism behind the EMC effect? The second is the concept of using the nucleus to study the process of hadron formation in high energy collisions. Both of these emphasize the importance of nuclear targets and are splendid examples of ways in which the nucleus can be used to provide insight into QCD. In order to concentrate on the physics issues, the discussion is qualitative. The quantitative backing does exist in the literature in the thorough studies of hadron fragmentation.

The explanations of the EMC effect described above seem to be conceptually rather different. Of course nature may have provided a mixture of such mechanisms. The most direct way to distinguish these processes would be a clean separation of the A dependence of the distributions of valence quarks (which carry the principal quantum numbers of the hadron) from that of the ocean quarks (quark-antiquark pairs produced by gluon interactions and vacuum polorization). The difficulty for the neutrino measurements which can do this in principle in a singles experiment lies in the absolute normalization, statistics, and the problems in using very heavy mass targets. This information can be inferred by measuring the coincident hadrons. Furthermore, the identification of the leading hadrons provides the opportunity to study the flavor dependence of the EMC effect.

The ideas are perhaps most simply visualized in configuration space. Figure 4 shows a conceptual diagram of radial dependences of the quark distributions. Whatever the detailed mechanism of confinement, the valence quarks are "confined" within the confinement region. The light ocean quarks, u, $\bar{u}$, d, $\bar{d}$ must extend out into the external region as they are the constituents of the meson cloud. There is no need that the transition through the confinement region be as smooth as that shown in Figure 4, the confinement region is a black box to this extent, but the distributions are indeed continuous. Inside a nucleus, the mutual nucleon-nucleon interactions will certainly affect the distributions of light ocean quarks. The increased pion content of the nucleus compared to an assemblage of free nucleons can be calculated from conventional nuclear theory.[12] However, the exchange of strange mesons is very weak in meson exchange models where kaon exchange must be at least a second order process and is further suppressed by the large kaon mass. The exchange of mesons with hidden strangeness such as the Φ is also reduced by large mass factors. This picture suggests that enhancements of the meson cloud should affect the light ocean quarks but not the heavier ocean quarks or the valence quarks. In contrast

ANL-P-17,876

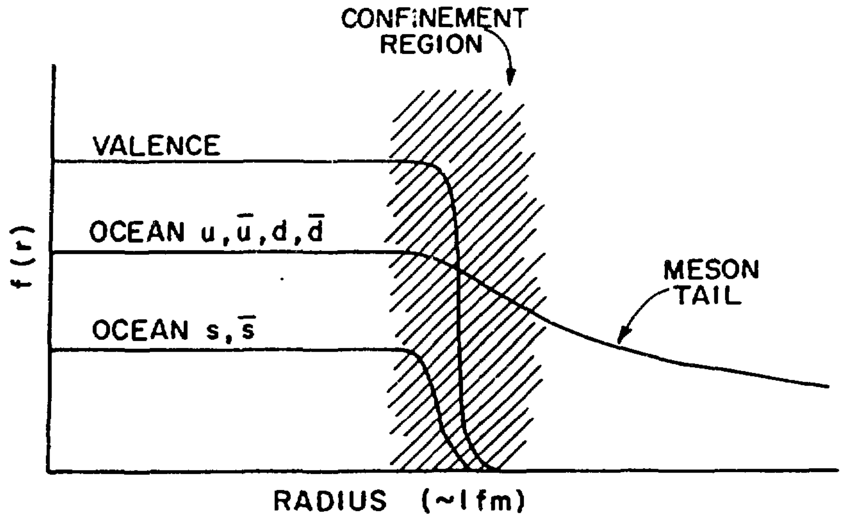

Figure 4 A schematic representative of the quark distributions in nuclei. No significance should be attached to the details of this particular representation which is based on bag models.

a change in the confinement process which changes the size of the nucleon in the nuclear medium may affect the distributions of all the quarks.

If one only looks at hadrons which emerge with a large fraction (>50%) of the momentum and energy of the virtual photon, then the chances are high that this hadron contains the struck quark. The identity of the hadron gives information as to which type of quark was struck. An emerging Φ which consists of an $s\bar{s}$ pair must be from the ocean of s and $\bar{s}$. Outgoing K^- ($\bar{u}s$) must be from the ocean, either a struck $\bar{u}$ or a struck s. The interaction of the photon is 4 times stronger with the charge 2/3 $\bar{u}$ than the charge 1/3 s, but the probability that the outgoing quark picks up a light quark in hadronization is roughly twice that for a heavier s quark.[13,14] (In a simple tunneling model[15] the probability of picking up a quark with mass m is ~ $\exp(-15\ M^2)$ giving a u:d:s:c ≈ $1:1:0.3:10^{-11}$). So the K^-'s are approximately twice as likely to be from the u ocean as from the s ocean. Similarly π^+'s and ρ^+'s ($u\bar{d}$) are weighted by a factor of four in favor of the struck quark being a valence or ocean u rather than an ocean $\bar{d}$. For π^+ in coincidence with muons at large x (x>.3), the valence distributions will be emphasized. The power of the coincidence technique is to permit the dissection of the flavor dependence of the EMC effect. In the simplest comparison of the rescaling and pion models, the valence and s quark distributions are not affected in the pion plus nucleon models, while all the distributions are affected if the structure of the nucleon changes. A word of warning is certainly in order here. One cannot extract the radial dependences of these quark distributions from the measured structure function, at least not in any model independent way. (If one could, then the long debated question of the size of the nucleon bag would be an easily settled experimental question.) Furthermore, one must take into account that many of the mesons arise from the decay of heavier resonances. This can provide significant corrections to the raw meson yields.

The second physical question is an example of how the nuclear medium can be used to study an important high energy process, namely hadronization in high-energy collisions. Conceptually the time evolution of the reaction is illustrated in Fig. 5. When the photon interacts with one of the quarks of the target, that quark absorbs the energy and momentum of the virtual photon. As it starts to leave the vicinity of the interaction the region of space occupied by the color singlet stretches and the centroids of color of the struck quark and remnant diquark separate. This is often dynamically described in terms of a string connecting the color centers with a given string tension.[15] As the string stretches, it eventually reaches a distance where it is more economical to polarize the vacuum and form hadrons. In principle and in detail there are questions about what limits the breaking of the string and how the momenta of the partons and string are divided in the resulting hadrons. Does, for example, each breaking of the string leave at least one physical hadron, or do the separate string fragments continue to break until the energy and momentum of the fragments become close enough to those of on-mass-shell particles that the fragments are stable? There is some mass or length scale ,L, over which the energy of the string builds which characterizes the breaking of the string. Simply due to the Lorentz dilation for the fast moving outgoing quark, this quark travels a distance is the laboratory of:

$$D = L\,\gamma = LE_{lab}/M \tag{3}$$

before the string breaks. The exact scale for this process is not well determined, but is approximately L≈.2 fm. Thus a 50-GeV quark may travel 10 fm before hadronization occurs.

These distance scales are quite comparable to the size of typical nuclear targets (the radius of ^{14}N is 2.6 fm and the radius of ^{132}Xe is 5.7 fm.) For high energy hadrons, hadronization takes places predominently outside of the nucleus, while for low energy hadrons the process takes place completely inside the nucleus. The flexible kinematics of the coincidence experiment allows the separation of these hadronization effects from the effects of changes in the quark structure functions on the original interaction. By varying Q^2 and the energy loss of the muon, one can look at leading hadrons at any E_{lab}. Fixing x fixes the quark structure functions while fixing E_{lab} fixes the hadronization effects.

There is no clear way to picture the effects of the propagation of the quark through the nuclear medium before hadronization takes

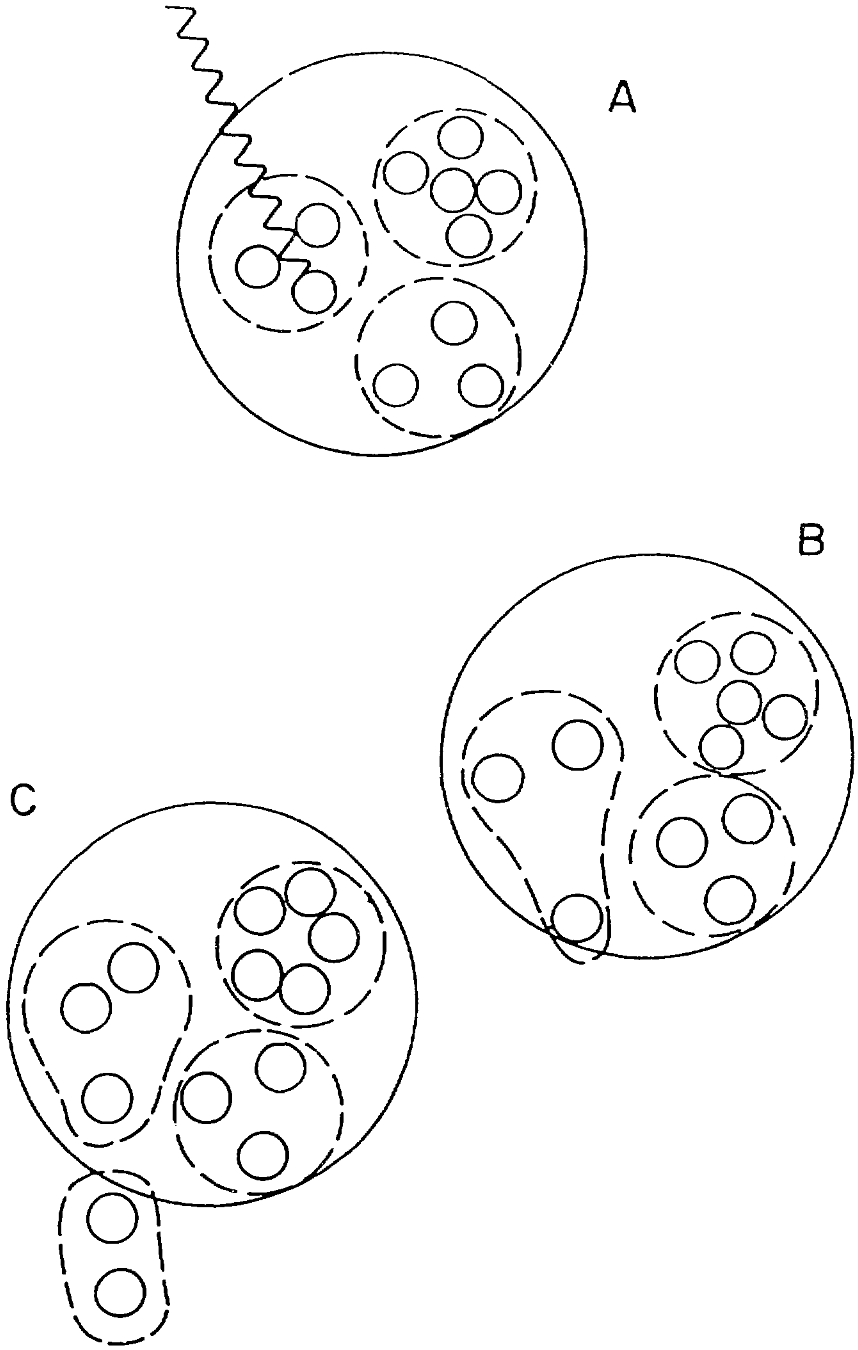

Figure 5 A conceptual picture of the three stages of hadron production in deep inelastic muon scattering. a) One quark in the target absorbs the energy and momentum of the virtual photon. b) The struck quark begins to propagate through the nucleus. The "string" connecting the color centers of the quark in the original nucleon stretches. c) The string breaks and a hadron forms.

place. Simple models[17] often consider this as the passage of a "free" quark and from the A dependence hope to extract the "quark-nucleon" interaction cross section and determine L, the scale of hadronization. It is quite conceivable that there is a dynamic polarization mechanism which could change the average string tension in the nucleus compared to that in free space. Hadronization is another manifestation of the essential confinement mechanism of QCD, and there are many possibilities for new phenomena to arise.

In summary , E665 promises to explore a number of fascinating aspects of quark degrees of freedom in nuclei. This one experiment can address issues in <u>perturbative</u> QCD, none of which have been discussed here, and in the nature of confinement. It will provide insight in the mechanism underlying the EMC effect and the dynamic formation of hadrons at high energy. Furthermore, the results will provide new information on hadron propagation in nuclei. In the next few months, the first tests of the muon beam line will take place. E665 is scheduled to begin taking data in December 1986. This experiment along with the SLAC measurements and high energy hadron measurements on nuclei will provide extremely valuable information on the quark structure of nuclei and will complement the precision measurements at lower momentum transfer to elucidate the importance of quark degrees of freedom in nuclear systems.

The authors would like to acknowledge valuable discussions with Fritz Coester on deep inelastic scattering and the EMC effort. Any weaknesses or errors in the presentation of the physics are solely the authors responsibility after ignoring his advice.

This research was supported by the U.S. Department of Energy under Contract W-31-109-ENG-38.

REFERENCES

1. European Muon Collaboration, J. J. Aubert et al., Phys. Lett. 123B, 275 (1983). EMC has been an extremely productive collaboration of scientists with more than a dozen publications on various aspects of deep inelastic muon scattering from nucleons and nuclei. A single reference certainly does not do justice to this important body of work.
2. A. Bodek et al., Phys. Rev. Lett. 50, 1431 (1983) and 51, 534 (1983).
3. R. G. Arnold et al., Phys. Rev. Lett. 52, 727 (1984).
4. Experiment 665 is a collaboration between Argonne, University of California at San Diego, CERN, Cracow, Fermilab, Freiburg, Harvard, University of Illinois at Chicago, Maryland, M. I. T., Max Planck Institute-Munich, Washington, Wuppertal and Yale. The spokesmen for the experiment are T. B. W. Kirk (FNAL) and V. Eckardt (MPI).
5. Bologna-CERN-Dubna-Munich-Saclay (BCDMS) Collaboration (CERN experiment NA4), as quoted by I. A. Savin, Rapporteur report, Int Conf. on High Energy Physics, Leipzig, July 1984
6. G. B. West to be published.
7. R. G. Arnold, Invited paper at this meeting.
8. F. E. Close et al. Phys. Lett. 129B, 346 (1983); F. E. Close et al. Phys. Rev. D31,1004(1985)
9. E. L. Berger and F. Coester, ANL preprint ANL-HEP-PR-84-97, to be published.
10. Additional neutrino measurements could, if performed with sufficient precision, determine the sea combination $x(\bar{u} + \bar{d} + 2\bar{s})$.
    The present neutrino data give a value of the ratio of the antiquark distributions in Fe compared to H of $1.10 \pm 0.11 \pm 0.07$. H. Abramowicz et al, Z. für Phys. 25, 29 (1984).
11. EMC, A. Arvidson et al., Nucl. Phys. B246, 381 (1984).

12. B. L. Friman, V. R. Pandharipande and R. B. Wiringa, Phys. Rev. Lett. 51, 763 (1983); F. Coester, Recent Progress in Many-Body Theories, Proc. Third. Int. Conf., Odentol-Altenberg, Germany, ed. by H. Kummel and M. L. Ristig (Lecture Notes in Physics, Springer-Verlag, 1984), Vol. 198, p. 16; R. B. Wiringa, R. A. Smith and T. L. Ainsworth, Phys. Rev. C29, 1207 (1984).

13. W. Bortel et al., Z. Phys. C20, 187 (1983).

14. B. Anderson and G. Gustafson, Z. Phys. C3, 223 (1980).

15. B. Anderson, G. Gustafson, G. Ingelmon and T. Sjöstrand, Phys. Rep. 97, 31 (1983); X. Artru, Phys. Rep. 97, 147 (1983).

16. J. D. Bjorken, SLAC-PUB-1796 (1976); N. N. Nikoloev, JETP Lett 22, 419 (1975).

17. A. Bialas and E. Bialas, Phys. Rev. D21, 675 (1980); A. Bialas, Act. A. Phys. Pol. 11, 475 (1980).